DNA-induced circularly polarized luminescence of helicene racemates

Fuwei Gan, Peng Yang, Juncong Liang, Chengshuo Shen, Jeanne Crassous, Huibin Qiu

▶ **To cite this version:**

Fuwei Gan, Peng Yang, Juncong Liang, Chengshuo Shen, Jeanne Crassous, et al.. DNA-induced circularly polarized luminescence of helicene racemates. Chirality, 2023, 10.1002/chir.23566 . hal-04087938

HAL Id: hal-04087938
https://hal.science/hal-04087938

Submitted on 13 May 2023

HAL is a multi-disciplinary open access archive for the deposit and dissemination of scientific research documents, whether they are published or not. The documents may come from teaching and research institutions in France or abroad, or from public or private research centers.

L'archive ouverte pluridisciplinaire **HAL**, est destinée au dépôt et à la diffusion de documents scientifiques de niveau recherche, publiés ou non, émanant des établissements d'enseignement et de recherche français ou étrangers, des laboratoires publics ou privés.

DNA-Induced Circularly Polarized Luminescence of Helicene Racemates

Fuwei Gan,[#1] Peng Yang,[#1] Juncong Liang,[1] Chengshuo Shen,*[1] Jeanne Crassous,*[2] and Huibin Qiu*[1]

Abstract: Enantiopure helicenes have been extensively investigated due to their outstanding chiroptical properties, while helicene racemates are considered as chiroptically silent. Here, we describe a facile method to produce circularly polarized luminescence (CPL) from helicene racemates via supramolecular association with DNA in aqueous solution. Racemic cationic helicene derivatives are immobilized in the grooves of commercially available double-stranded right-handed DNA, and the discrimination of left- and right-handed helicenes by chiral DNA is monitored by single molecule force spectroscopy. This subsequently leads to the generation of prominent CPL with dissymmetric factor $|g_{lum}|$ of close to 0.01, which is approximate to enantiopure helicenes. The strategy developed in this work avoids the tedious and expensive chiral resolution process, and provides a distinctive insight into the fabrication of CPL-emitting systems.

Keywords: DNA, helicene, circularly polarized luminescence, single molecular force spectroscopy

1 Introduction

Materials with dissymmetric generation of left- and right-handed circularly polarized luminescence (CPL)[1,2] are highly useful for a rich array of applications, such as 3D optical display,[3,4] information storage and processing,[5,6] photoelectric devices,[7–9] and optical security tags.[10] So far, it remains a significant challenge to produce CPL with high dissymmetry factor (g_{lum}), majorly due to the rare existence of a system with large magnetic dipole moment and relatively small electric dipole moment within electron transitions during the emission process. Only a few categories of small chiral organic molecules,[8,11,12] such as paracyclophanes,[13,14] helicenes[15–25] and BINOL derivatives,[26–30] could produce obvious CPL with relatively high $|g_{lum}|$ in the range of 10^{-3} ~ 10^{-2}. Several types of chiral lanthanide complexes possess larger $|g_{lum}|$ (0.05 to 1.38) due to the unique intraconfiguration *f-f* transitions which are Laporte-forbidden and display large rotatory strength.[31–33] However, the application of these lanthanide CPL materials is normally limited due to their low luminescence intensity, as well as the difficulties in molecular design and synthesis.

Generally, conventional study on CPL performance involves the use of enantiopure materials, while racemic compounds are considered as CPL silent. In most cases, chiral resolution is necessary to obtain the enantiomers for further CPL investigation and this raises critical issues due to the high cost using preparative HPLC or the sophisticated process using crystallization-driven spontaneous resolution.[18] Combining achiral luminophores and readily available chiral molecules (e.g., amino acids and their derivatives) through covalent bonds[34,35] or supramolecular interaction[36–46] to form structurally chiral supramolecular system is emerging as a promising approach to produce CPL. However, these systems highly depend on the pre-assembled supramolecular structures, which brings considerable limitation in actual applications. Besides, the $|g_{lum}|$ is usually limited within the range of 10^{-4} ~ 10^{-2}. It was also demonstrated that DNA or protein could noncovalently associate and selectively recognize helicene enantiomers.[47–54] However, so far there is no investigation focusing on the CPL properties of these biomolecule/helicene complexes. Herein, we develop a distinctive method for helicene racemates to generate intense CPL with high $|g_{lum}|$ that is comparable with enantiopure helicenes, simply by supramolecular association with commercially available double-stranded DNA (ds-DNA). This avoids the tedious chiral resolution process and thus enables a facile use of helicene derivatives in the fields of chiroptical devices.

2 Materials and Methods

2.1 Synthesis of azahelicenes and azahelicenia

Racemic 4-aza[6]helicene (*rac*-[6]H, CCDC number: 2204488) and racemic 4-aza[7]helicene (*rac*-[7]H, CCDC number: 2204492) were synthesized via photocyclization and subsequently transformed to water-soluble helicenium salts, namely, *rac*-[6]H$^+$·I$^-$ and *rac*-[7]H$^+$·I$^-$ (Figure 1a), by quaternization with iodomethane (see Supporting Information for synthetic procedures and characterization details). Enantiopure *P*- and *M*-[6]H, and *P*- and *M*-[7]H were obtained by chiral resolution via HPLC. *P*- and *M*-[6]H$^+$·I$^-$, and *P*- and *M*-[7]H$^+$·I$^-$ were prepared by subsequent quaternization as well. Correspondingly, planar polyaromatic salts, i.e., [2]Q$^+$·I$^-$, [3]Q$^+$·I$^-$ and [4]Q$^+$·I$^-$ were also synthesized through quaternization for comparison (Figure 1b). These cationic salts show distinct luminescent colors in aqueous solution depending on the number of the aromatic rings (Figure 1).

[1]School of Chemistry and Chemical Engineering, Zhangjiang Institute for Advanced Study, Frontiers Science Center for Transformative Molecules, State Key Laboratory of Metal Matrix Composites, Shanghai Jiao Tong University, Shanghai 200240, People's Republic of China

[2]Institut des Sciences Chimiques de Rennes, UMR 6226, Campus de Beaulieu, CNRS-Université de Rennes 1, 35042 Rennes Cedex, France.

#F. Gan and P. Yang contributed equally to this work.

Correspondence
E-mail: hbqiu@sjtu.edu.cn
E-mail: shenchengshuo@zstu.edu.cn
E-mail: jeanne.crassous@univ-rennes1.fr

Received: ((will be filled in by the editorial staff))
Revised: ((will be filled in by the editorial staff))
Published online: ((will be filled in by the editorial staff))

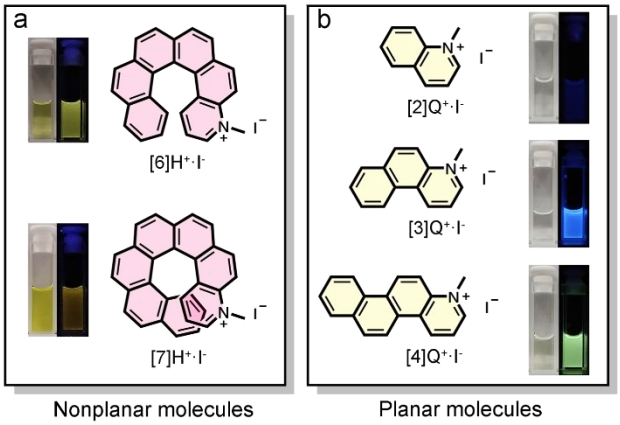

FIGURE 1 Molecular structures of (a) nonplanar helicenia and (b) planar polyaromatic salts used in this work and corresponding photographs of their aqueous solutions under visible and UV lights.

2.2 Supramolecular association

For supramolecular association, aqueous solutions of the above polyaromatic salts (c = 4 × 10^{-4} mol·L^{-1}) and commercially available long chain right-handed DNA (~2000 b.p., 1.0 mg·L^{-1}, $c_{b.p.}$ = 1.6 × 10^{-3} mol·L^{-1}, b.p. for base pair) were mixed in various volume ratios, with the final concentration of DNA fixed to 0.5 mg·L^{-1} (by adding a complementary amount of water). The resulting aqueous solutions of the complexes were used for the investigation of chiroptical properties. In control experiments, anionic chiral monomer disodium adenosine monophosphate (AMP) and short chain double-stranded DNA (< 50 b.p.) were used to take the place of the long chain double-stranded DNA.

3 Results and Discussion

As shown in Figure 2a, electronic circular dichroism (ECD) spectrum of native DNA presented a negative peak at 245 nm and a positive peak at 275 nm, which is representative for right-handed ds-DNA.[55] For the DNA/*rac*-[6]H^+·I^- complex, three positive ECD bands appeared at λ = 338, 382 and 464 nm along with a negative band at λ = 364 nm, corresponding to the absorption bands of *rac*-[6]H^+·I^-, which is beyond the absorption region of DNA (Figure 2a, inserted curves). The DNA/*rac*-[7]H^+·I^- complex showed analogous induced ECD signals at λ = 328, 349 and 412 nm (Figure 2a, inserted curves). Notably, DNA maintained its specific right-handed helical conformation during the association as the ECD bands around 260 nm almost retained the original shape (Figure 2a).

Interestingly, the DNA/*rac*-[6]H^+·I^- complex emitted intense negative CPL with g_{lum} of -0.009 at 540 nm when excited at 380 nm (Figure 2b). The DNA/*rac*-[7]H^+·I^- complex also showed strong negative CPL with g_{lum} of -0.008 at 560 nm (Figure 2b). This was comparable to the performance of enantiopure helicenia (g_{lum} = +0.016 and -0.015 at 565 nm for *P*- and *M*-[6]H^+·I^-, respectively, Figure S29 in SI; g_{lum} = +0.014 and -0.015 at 580 nm for *P*- and *M*-[7]H^+·I^-, respectively, Figure S30 in SI). Note that such $|g_{lum}|$ values of *ca*. 10^{-2} are fairly high for organic chiral emissive molecules.[8,11]

In order to clarify the effect of the helical molecular structure, we investigated the complexes derived from achiral planar molecules, including [2]Q·I^-, [3]Q·I^- and [4]Q·I^-. The DNA/[2]Q^+·I^- and DNA/[3]Q^+·I^- complexes were ECD silent at the wavelength longer than 300 nm (Figures S20 and S21), while the DNA/[4]Q^+·I^- complex presented two induced ECD bands at 324 and 417 nm (Figure S22 in SI). However, for all these complexes, no obvious CPL signal was detected in spite of the strong fluorescence generated by UV light irradiation (Figure 2b). It appeared that the nonplanar helical structures of helicenia are essential for the generation of CPL.

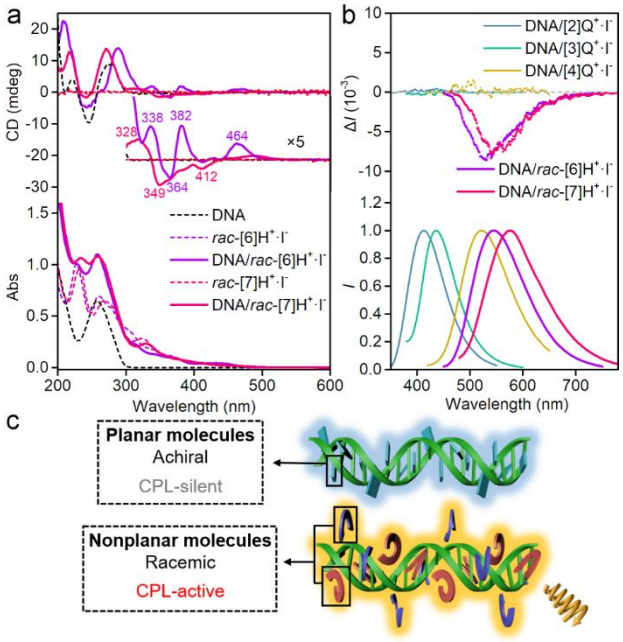

FIGURE 2 (a) UV-vis and ECD spectra of native DNA, *rac*-[6]H^+·I^-, *rac*-[7]H^+·I^-, and DNA/*rac*-[6]H^+·I^- and DNA/*rac*-[7]H^+·I^- complexes (c = 2 × 10^{-4} mol·L^{-1} for the azahelicenium moieties). (b) Fluorescent and CPL spectra of DNA/*rac*-[6]H^+·I^-, DNA/*rac*-[7]H^+·I^-, and DNA/[*n*]Q^+·I^- complexes (c = 2 × 10^{-4} mol·L^{-1} for the azahelicenium and [*n*]Q^+·I^- moieties, n = 2, 3, 4). (c) Schematic representations for the CPL performance of the above DNA complexes derived from planar and nonplanar molecules.

Subsequently, the interaction between DNA and helicenia was studied by single molecular force spectroscopy. The responding force-distance (*F-D*) curves showed that the pure DNA gave a constant force plateau up to 65 pN upon stretching (Figure 3a), which corresponds to its B-S transition[56,57]. When treated by helicenia with increasing concentrations, the force plateau gradually disappeared in the relative low force region, indicating a significant increase of the length of DNA. These results unambigously indicated that helicenia interact with DNA by intercalating into the base pairs.[58] Notably, for *P*- and *M*-helicenia, the dependence of *F-D* curve on the concentration was quite different. As shown in Figure 3b and 3c, the force-dependent binding constant (K_F) for the binding of DNA with the *P*-helicenia were constantly higher than the *M*-helicenia. Binding constant at zero force (K_0) was further used to describe the binding interaction between DNA and enantiomers. For *P*-[6]H^+·I^-, the K_0 value was calculated to be 1.9 × 10^4 M^{-1}, which was larger than that of *M*-[6]H^+·I^- (1.1 × 10^4 M^{-1}). Apparently, the binding interaction between DNA and *P*-[6]H^+·I^- was more intense, indictating an interesting enantioselectivity of DNA for the helicenia enantiomers. Similarly, the K_0 of *P*-[7]H^+·I^- (9.2 × 10^3 M^{-1}) was also higher than that of *M*-[7]H^+·I^- (3.7 × 10^3 M^{-1}). It indicated that the enantioselectivity of DNA towards the two enantiomers plays a important role in inducing ECD and CPL signals.

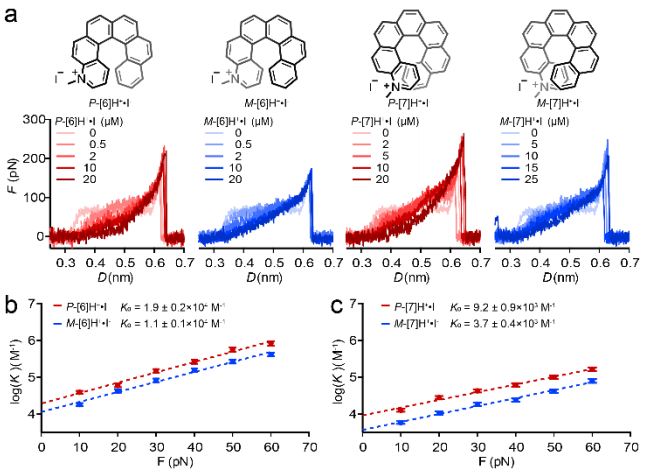

FIGURE 3 Enantioselectivity for the association of DNA with helicenia revealed by single molecular force spectroscopy. (a) Typical DNA stretching curves in the presence of *P*-[6]H$^+$·I$^-$, *M*-[6]H$^+$·I$^-$, *P*-[7]H$^+$·I$^-$, *M*-[7]H$^+$·I$^-$ with various concentrations. (b) and (c) Plot of binding constant at various force. Each point is determined from the fits (Figure S33 in SI), and lines are fit according to equation 2 (see supporting information, SI). The red and blue lines are the force-dependent binding constant of *P*- and *M*-helicenia with DNA, respectively.

We further investigated the chiroptical properties of the complexes formed by DNA and helicenia enantiomers. The mirror-imaged symmetry broke for the ECD spectra of DNA/*P*-[6]H$^+$·I$^-$ and DNA/*M*-[6]H$^+$·I$^-$ complexes (Figure 4a) and the mathematic average signal was no longer zero, while the resulting curve matched well with the ECD spectrum of the DNA/*rac*-[6]H$^+$·I$^-$ complex (Figure 4b). This again indicated a specific association differentiation for DNA towards *P*- and *M*-helicenia. Regarding the luminescence spectra, remarkable blue shifts (~ 20 nm, compared to free *P*- or *M*-[6]H$^+$·I$^-$) were observed for the DNA/*P*- and *M*-[6]H$^+$·I$^-$ complexes, which were probably caused by restricted geometric relaxation and freezing of low-frequency out-of-plane vibrations.[59–61] Importantly, this association differentiation also strongly affected the luminescence performance. The DNA/*P*- and *M*-[6]H$^+$·I$^-$ complexes exhibited apparently different strength of luminescence, with 30% and 44% of intensity (compared with free *P*- or *M*-[6]H$^+$·I$^-$) retained, respectively (Figure 4c, lower curves). Probably as a consequence of the quenching from the formation of excimers with strong π-π interaction, the luminescence intensity of helicenia decreased upon association with DNA. Relative to the DNA/*M*-[6]H$^+$·I$^-$ complex, DNA/*P*-[6]H$^+$·I$^-$ suffer more from fluorescence quenching. This also indicates that DNA prefers to binding with *P*-helicenia, which is consistent with the single molecular force spectroscopy experiments. Similar behaviour was also observed in the [7]H$^+$·I$^-$ system (Figure S31 in SI).

As for the CPL properties, it was found that the $|g_{lum}|$ of the complexes consist of enantiopure helicenia and DNA was considerably enhanced compared to free helicenia. The g_{lum} increased from +0.016 to +0.023 (540 nm) for *P*-[6]H$^+$·I$^-$, (Figure 4b, upper curves), and more obviously, from +0.014 to +0.057 (560 nm) for *P*-[7]H$^+$·I$^-$ (Figure S31 in SI). The *P*- and *M*-type complexes showed comparable $|g_{lum}|$ values (g_{lum} = -0.024 and -0.055 for DNA/*M*-[6]H$^+$·I$^-$ and DNA/*M*-[7]H$^+$·I$^-$, respectively, Figure 4c and Figure S31 in SI). Consequently, with the combination of these two effects (luminescence quenching and $|g_{lum}|$ enhancement), the contribution of the *M*-type complex for CPL activity surpasses the *P*-type analogue (Figure 4c, dark blue shading), and hence, the DNA/*rac*-helicenium complex presented negative CPL signals (Figure 2b). The induced CPL can thus be ascribed to the enantioselective association of DNA towards enantiopure helicenia, which is largely dependent on the nonplanar helical aromatic structure. It seemed quite different from the traditional CPL-active systems where planar achiral fluorophores were normally employed.[38–46]

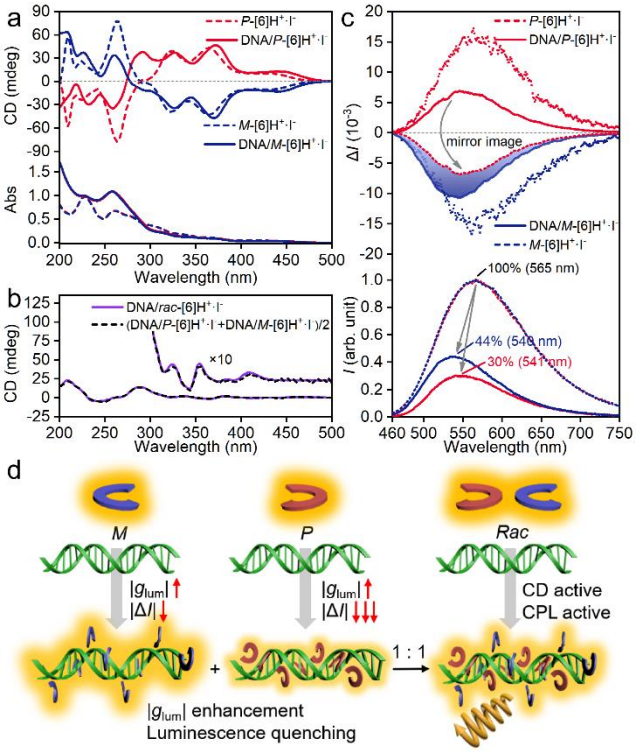

FIGURE 4 (a) UV-vis and ECD spectra of *P*- and *M*-[6]H$^+$·I$^-$, and DNA/*P*-[6]H$^+$·I$^-$ and DNA/*M*-[6]H$^+$·I$^-$ complexes ($c_{[6]H^+\cdot I^-}$ = 2 × 10^{-4} mol·L^{-1}). (b) ECD spectrum of DNA/*rac*-[6]H$^+$·I$^-$ complexes ($c_{[6]H^+\cdot I^-}$ = 2 × 10^{-4} mol·L^{-1}) and the average curve of the ECD spectra of DNA/*P*-[6]H$^+$·I$^-$ and DNA/*M*-[6]H$^+$·I$^-$ complexes. (c) Corresponding Fluorescence (The fluorescence intensity of free [6]H$^+$·I$^-$ is normalized as 100%; the fluorescence intensity of the DNA/helicenia complexes is calculated relative to free [6]H$^+$·I$^-$) and CPL spectra (Δ*I* of DNA/helicenia complexes is calculated according to the fluorescence intensity). (d) Schematic representations for the CPL performance and the origin of induced CPL as a result of both luminescence quenching and $|g_{lum}|$ enhancement.

Further experiments demonstrate that the right-handed helical secondary structure of DNA was also essential for the induced CPL. The complexes constructed from AMP or short chain double-stranded DNA showed nearly no ECD signal in the absorption region of azahelicenia (300–500 nm) (Figures S23 and S24). In addition, the induced ECD signal decreased or even disappeared after destroying the double-stranded helical structure of DNA by mixing the complexes with NaOH (Figures S25 and S26). CPL spectra showed similar tendency as small chiral molecule AMP, short chain DNA and denatured long chain DNA were unable to induce CPL of racemic helicenia (Figure 5 and Figure S32 in SI). These results demonstrated that the structural chirality of ds-DNA rather than the molecular chirality generates the induced ECD and CPL of racemic helicenia.

Conclusion

In summary, we have established a facile method to generate considerable CPL ($|g_{lum}|$ ~ 0.01) based on commercially available right-handed ds-DNA and racemic helicene derivatives. Single molecular force spectroscopy and chiroptical spectroscopy revealed that DNA binds more intensively to *P*-helicenia than *M*-helicenia. The diastereoselective supramolecular association along with the differentiated luminescence quenching and the enhanced $|g_{lum}|$ are essential for

the induced CPL of racemic helicenia. We are currently exploring a series of emissive helicene and curved nanographene derivatives in racemic form to fabricate novel CPL-emitting materials, as well as to seek potential applications in soft devices (e.g., OLED or OFET).

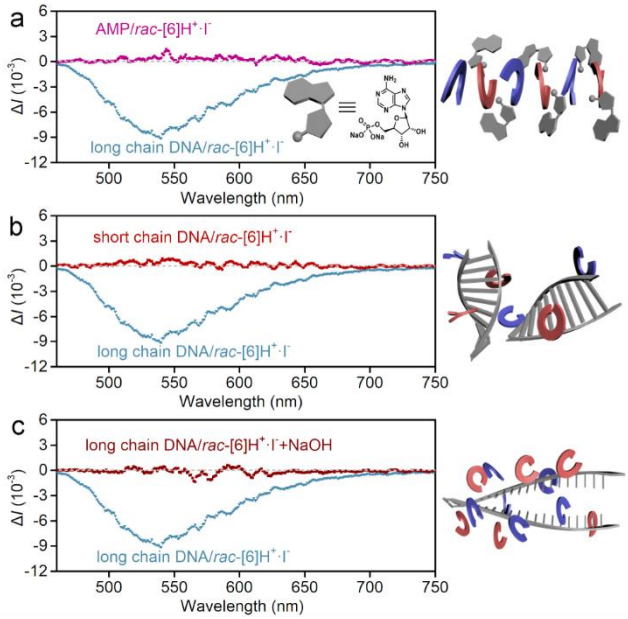

FIGURE 5 (a) CPL spectra of above-mentioned long chain DNA/$[6]H^+{\cdot}I^-$ complex and AMP/$[6]H^+{\cdot}I^-$ complex ($c_{[6]H^+{\cdot}I^-}$ = 2 × 10^{-4} mol·L^{-1}, c_{AMP} = 0.5 mg·mL^{-1}). (b) CPL spectra of above-mentioned long chain DNA/$[6]H^+{\cdot}I^-$ complex and short chain DNA/$[6]H^+{\cdot}I^-$ complex ($c_{[6]H^+{\cdot}I^-}$ = 2 × 10^{-4} mol·L^{-1}). (c) CPL spectra of DNA/$[6]H^+{\cdot}I^-$ complex in the absence and presence of NaOH ($c_{[6]H^+{\cdot}I^-}$ = 2 × 10^{-4} mol·L^{-1}, c_{NaOH} = 2 × 10^{-2} mol·L^{-1}). The sketches show the possible interaction models.

Acknowledgements

This work was financially supported by the National Key R&D Program of China (2020YFA0908100), the National Natural Science Foundation of China (92056110, 22075180), the Innovation Program of Shanghai Municipal Education Commission (202101070002E00084), the Science and Technology Commission of Shanghai Municipality (20JC1415000, 21XD1421900).

Supporting information

Additional supporting information may be found in the online version of this article at the publisher's website.

REFERENCES

1. Richardson FS, Riehl JP. Circularly polarized luminescence spectroscopy. *Chem Rev.* 1977;77(6):773–792.
2. Riehl JP, Richardson FS. Circularly polarized luminescence spectroscopy. *Chem Rev.* 1986;86(1):1–16.
3. Schadt M. LIQUID CRYSTAL MATERIALS AND LIQUID CRYSTAL DISPLAYS. *Annu Rev Mater Sci.* 1997;27(1):305–379.
4. Zinna F, Giovanella U, Bari LD. Highly circularly polarized electroluminescence from a chiral europium complex. *Adv Mater.* 2015;27(10):1791–1795.
5. Sherson JF, Krauter H, Olsson RK, Julsgaard B, Hammerer K, Cirac I, Polzik ES. Quantum teleportation between light and matter. *Nature.* 2006;443(7111):557–560.
6. Wagenknecht C, Li C-M, Reingruber A, Bao X-H, Goebel A, Chen Y-A, Zhang Q, Chen K, Pan J-W. Experimental demonstration of a heralded entanglement source. *Nat Photonics.* 2010;4(8):549–552.
7. Yang Y, da Costa RC, Fuchter MJ, Campbell AJ. Circularly polarized light detection by a chiral organic semiconductor transistor. *Nat Photonics.* 2013;7(8):634–638.
8. Sánchez-Carnerero EM, Agarrabeitia AR, Moreno F, Maroto BL, Muller G, Ortiz MJ, de la Moya S. Circularly polarized luminescence from simple organic molecules. *Chem Eur J.* 2015;21(39):13488–13500.
9. Han J, Duan P, Li X, Liu M. Amplification of circularly polarized luminescence through triplet–triplet annihilation-based photon upconversion. *J Am Chem Soc.* 2017;139(29):9783–9786.
10. Carr R, Evans NH, Parker D. Lanthanide complexes as chiral probes exploiting circularly polarized luminescence. *Chem Soc Rev.* 2012;41(23):7673–7686.
11. Tanaka H, Inoue Y, Mori T. Circularly polarized luminescence and circular dichroisms in small organic molecules: Correlation between Excitation and Emission Dissymmetry Factors. *ChemPhotoChem.* 2018;2(5):386–402.
12. Han J, Guo S, Lu H, Liu S, Zhao Q, Huang W. Recent progress on circularly polarized luminescent materials for organic optoelectronic devices. *Adv Optical Mater.* 2018;6(17):1800538.
13. Morisaki Y, Gon M, Sasamori T, Tokitoh N, Chujo Y. Planar chiral tetrasubstituted [2.2]paracyclophane: optical resolution and functionalization. *J Am Chem Soc.* 2014;136(9):3350–3353.
14. Gon M, Morisaki Y, Chujo Y. Optically active cyclic compounds based on planar chiral [2.2]paracyclophane: extension of the conjugated systems and chiroptical properties. *J Mater Chem C.* 2015;3(3):521–529.
15. Field JE, Muller G, Riehl JP, Venkataraman D. Circularly polarized luminescence from bridged triarylamine helicenes. *J Am Chem Soc.* 2003;125(39):11808–11809.
16. Sawada Y, Furumi S, Takai A, Takeuchi M, Noguchi K, Tanaka K. Rhodium-catalyzed enantioselective synthesis, crystal structures, and photophysical properties of helically chiral 1,1′-bitriphenylenes. *J Am Chem Soc.* 2012;134(9):4080–4083.
17. Oyama H, Nakano K, Harada T, Kuroda R, Naito M, Nobusawa K, Nozaki K. Facile synthetic route to highly luminescent sila[7]helicene. *Org Lett.* 2013;15(9):2104–2107.
18. Shen C, Anger E, Srebro M, Vanthuyne N, Deol KK, Jefferson TD, Muller G, Williams JAG, Toupet L, Roussel C and others. Straightforward access to mono- and bis-cycloplatinated helicenes displaying circularly polarized phosphorescence by using crystallization resolution methods. *Chem Sci.* 2014;5(5):1915–1927.
19. Dhbaibi K, Favereau L, Srebro-Hooper M, Jean M, Vanthuyne N, Zinna F, Jamoussi B, Di Bari L, Autschbach J, Crassous J. Exciton coupling in diketopyrrolopyrrole–helicene derivatives leads to red and near-infrared circularly polarized luminescence. *Chem Sci.* 2018;9(3):735–742.20.
21. Goto K, Yamaguchi R, Hiroto S, Ueno H, Kawai T, Shinokubo H. Intermolecular oxidative annulation of 2-aminoanthracenes to diazaacenes and aza[7]helicenes. *Angew Chem Int Ed.* 2012;51(41):10333–10336.
22. Nakamura K, Furumi S, Takeuchi M, Shibuya T, Tanaka K. Enantioselective synthesis and enhanced circularly polarized luminescence of S-shaped double azahelicenes. *J Am Chem Soc.* 2014;136(15):5555–5558.
23. Mendola D, Saleh N, Vanthuyne N, Roussel C, Toupet L, Castiglione F, Caronna T, Mele A, Crassous J. Aza[6]helicene platinum complexes: chirality control of *cis–trans* Isomerism. *Angew Chem Int Ed.* 2014;53(23):5786–5790.
24. Ushiyama A, Hiroto S, Yuasa J, Kawai T, Shinokubo H. Synthesis of a figure-eight azahelicene dimer with high emission and CPL properties. *Org Chem Front.* 2017;4(5):664–667.
25. Otani T, Tsuyuki A, Iwachi T, Someya S, Tateno K, Kawai H, Saito T, Kanyiva KS, Shibata T. Facile two-step synthesis of 1,10-phenanthroline-derived polyaza[7]helicenes with high fluorescence and CPL efficiency. *Angew Chem Int Ed.* 2017;56(14):3906–3910.

26. Sánchez-Carnerero EM, Moreno F, Maroto BL, Agarrabeitia AR, Ortiz MJ, Vo BG, Muller G, Moya Sdl. Circularly polarized luminescence by visible-light absorption in a chiral *O*-BODIPY dye: unprecedented design of CPL organic molecules from achiral chromophores. *J Am Chem Soc.* 2014;136(9):3346–3349.
27. Zhang S, Wang Y, Meng F, Dai C, Cheng Y, Zhu C. Circularly polarized luminescence of AIE-active chiral *O*-BODIPYs induced via intramolecular energy transfer. *Chem Commun.* 2015;51(43):9014–9017.
28. Feuillastre S, Pauton M, Gao L, Desmarchelier A, Riives AJ, Prim D, Tondelier D, Geffroy B, Muller G, Clavier G and others. Design and synthesis of new circularly polarized thermally activated delayed fluorescence emitters. *J Am Chem Soc.* 2016;138(12):3990–3993.
29. Takaishi K, Yamamoto T, Hinoide S, Ema T. helical oligonaphthodioxepins showing intense circularly polarized luminescence (CPL) in solution and in the solid state. *Chem Eur J.* 2017;23(39):9249–9252.
30. Sun Z-B, Liu J-K, Yuan D-F, Zhao Z-H, Zhu X-Z, Liu D-H, Peng Q, Zhao C-H. 2,2′-Diamino-6,6′-diboryl-1,1′-binaphthyl: a versatile building block for temperature-dependent dual fluorescence and switchable circularly polarized luminescence. *Angew Chem Int Ed.* 2019;58(15):4840–4846.
31. Lunkley JL, Shirotani D, Yamanari K, Kaizaki S, Muller G. Extraordinary circularly polarized luminescence activity exhibited by cesium tetrakis(3-heptafluoro-butylryl-(+)-camphorato) Eu(III) complexes in EtOH and $CHCl_3$ solutions. *J Am Chem Soc.* 2008;130(42):13814–13815.
32. Muller G. Luminescent chiral lanthanide(III) complexes as potential molecular probes. *Dalton Trans.* 2009(44):9692–9707.
33. Zinna F, Di Bari L. Lanthanide circularly polarized luminescence: bases and applications. *Chirality.* 2015;27(1):1–13.
34. Kumar J, Nakashima T, Kawai T. Circularly polarized luminescence in chiral molecules and supramolecular assemblies. *J Phys Chem Lett.* 2015;6(17):3445–3452.
35. Roose J, Tang BZ, Wong KS. Circularly-polarized luminescence (CPL) from chiral AIE molecules and macrostructures. *Small.* 2016;12(47):6495–6512.
36. Huo S, Duan P, Jiao T, Peng Q, Liu M. Self-assembled luminescent quantum dots to generate full-color and white circularly polarized light. *Angew Chem Int Ed.* 2017;56(40):12174–12178.
37. Shi Y, Duan P, Huo S, Li Y, Liu M. Endowing perovskite nanocrystals with circularly polarized luminescence. *Adv Mater.* 2018;30(12):1705011.
38. Wang Y, Li X, Li F, Sun W-Y, Zhu C, Cheng Y. Strong circularly polarized luminescence induced from chiral supramolecular assembly of helical nanorods. *Chem Commun.* 2017;53(54):7505–7508.
39. Goto T, Okazaki Y, Ueki M, Kuwahara Y, Takafuji M, Oda R, Ihara H. Induction of strong and tunable circularly polarized luminescence of nonchiral, nonmetal, low-molecular-weight fluorophores using chiral nanotemplates. *Angew Chem Int Ed.* 2017;56(11):2989–2993.
40. Yang D, Duan P, Zhang L, Liu M. Chirality and energy transfer amplified circularly polarized luminescence in composite nanohelix. *Nat Commun.* 2017;8(1):15727.
41. Han J, You J, Li X, Duan P, Liu M. Full-color tunable circularly polarized luminescent nanoassemblies of achiral AIEgens in confined chiral nanotubes. *Adv Mater.* 2017;29(19):1606503.
42. Han D, Han J, Huo S, Qu Z, Jiao T, Liu M, Duan P. Proton triggered circularly polarized luminescence in orthogonal- and co-assemblies of chiral gelators with achiral perylene bisimide. *Chem Commun.* 2018;54(44):5630–5633.
43. Jiang H, Jiang Y, Han J, Zhang L, Liu M. Helical nanostructures: chirality transfer and a photodriven transformation from superhelix to nanokebab. *Angew Chem Int Ed.* 2019;58(3):785–790.
44. Ji L, Sang Y, Ouyang G, Yang D, Duan P, Jiang Y, Liu M. Cooperative chirality and sequential energy transfer in a supramolecular light-harvesting nanotube. *Angew Chem Int Ed.* 2019;58(3):844–848.
45. Hu L, Li K, Shang W, Zhu X, Liu M. Emerging cubic chirality in γCD-MOF for fabricating circularly polarized luminescent crystalline materials and the size effect. *Angew Chem Int Ed.* 2020;59(12):4953–4958.
46. Kazem-Rostami M, Orte A, Ortuño AM, David AHG, Roy I, Miguel D, Garci A, Cruz CM, Stern CL, Cuerva JM and others. Helically chiral hybrid cyclodextrin Metal–Organic Framework exhibiting circularly polarized luminescence. *J Am Chem Soc.* 2022;144(21):9380–9389.
47. Honzawa S, Okubo H, Anzai S, Yamaguchi M, Tsumoto K, Kumagai I. Chiral recognition in the binding of helicenediamine to double strand DNA: interactions between low molecular weight helical compounds and a helical polymer. *Bioorg Med Chem.* 2002;10(10):3213–3218.
48. Xu Y, Zhang YX, Sugiyama H, Umano T, Osuga H, Tanaka K. (*P*)-helicene displays chiral selection in binding to Z-DNA. *J Am Chem Soc.* 2004;126(21):6566–6567.
49. Shinohara K-i, Sannohe Y, Kaieda S, Tanaka K-i, Osuga H, Tahara H, Xu Y, Kawase T, Bando T, Sugiyama H. A Chiral wedge molecule inhibits telomerase activity. *J Am Chem Soc.* 2010;132(11):3778–3782.
50. Tsuji G, Kawakami K, Sasaki S. Enantioselective binding of chiral 1,14-dimethyl[5]helicene–spermine ligands with B- and Z-DNA. *Bioorg Med Chem.* 2013;21(19):6063–6068.
51. Kawara K, Tsuji G, Taniguchi Y, Sasaki S. Synchronized chiral induction between [5]helicene–spermine ligand and B–Z DNA transition. *Chem Eur J.* 2017;23(8):1763–1769.
52. Zhou Y, Gan F, Zhang Y, He X, Shen C, Qiu H, Liu P. Selective killing of cancer cells by nonplanar aromatic hydrocarbon-induced DNA damage. *Adv Sci.* 2019;6(21):1901341.
53. He X, Gan F, Zhou Y, Zhang Y, Zhao P, Zhao B, Tang Q, Ye L, Bu J, Mei J and others. Nonplanar helicene benzo[4]helicenium for the precise treatment of renal cell carcinoma. *Small Methods.* 2021;5(11):2100770.
54. Lousen B, Pedersen SK, Răsădean DM, Pantoş GD, Pittelkow M. Triggering G-quadruplex conformation switching with [7]helicenes. *Chem Eur J.* 2021;27(19):6064–6069.
55. Sprecher CA, Baase WA, Johnson Jr. WC. Conformation and circular dichroism of DNA. *Biopolymers.* 1979;18(4):1009–1019.
56. Smith SB, Cui Y, Bustamante C. Overstretching B-DNA: The elastic response of individual double-stranded and single-stranded DNA molecules. *Science.* 1996;271(5250):795–799.
57. Lai P-Y, Zhou Z. B- to S-form transition in double-stranded DNA with basepair interactions. *Physica A.* 2003;321(1):170–180.
58. Vladescu ID, McCauley MJ, Nuñez ME, Rouzina I, Williams MC. Quantifying force-dependent and zero-force DNA intercalation by single-molecule stretching. *Nat Methods.* 2007;4(6):517–522.
59. He J, Xu B, Chen F, Xia H, Li K, Ye L, Tian W. Aggregation-induced emission in the crystals of 9,10-distyrylanthracene derivatives: the essential role of restricted intramolecular torsion. *J Phys Chem C.* 2009;113(22):9892–9899.
60. Wu Q, Zhang T, Peng Q, Wang D, Shuai Z. Aggregation induced blue-shifted emission – the molecular picture from a QM/MM study. *Phys Chem Chem Phys.* 2014;16(12):5545–5552.
61. Virk TS, Ilawe NV, Zhang G, Yu CP, Wong BM, Chan JMW. Sultam-based hetero[5]helicene: synthesis, structure, and crystallization-induced emission enhancement. *ACS Omega.* 2016;1(6):1336–1342.

Graphical Abstract